Front. Eng. Manag. 2024, 11(4): 645–660
https://doi.org/10.1007/s42524-024-3088-9

RESEARCH ARTICLE

Kang HUANG, Feixiong LIAO, Soora RASOULI, Ziyou GAO

Toward energy-efficient urban rail transit with capacity constraints under a public health emergency

Abstract Urban rail transit (URT) plays a pivotal role in mitigating urban congestion and emissions, positioning it as a sustainable transportation alternative. Nevertheless, URT's function in transporting substantial numbers of passengers within confined public spaces renders it vulnerable to the proliferation of infectious diseases during public health crises. This study proposes a decision support model that integrates operational control strategies pertaining to passenger flow and train capacity utilization, with an emphasis on energy efficiency within URT networks during such crises. The model anticipates a URT system where passengers adhere to prescribed routes, adhering to enhanced path flow regulations. Simultaneously, train capacity utilization is intentionally limited to support social distancing measures. The model's efficacy was assessed using data from the COVID-19 outbreak in Xi'an, China, at the end of 2021. Findings indicate that focused management of passenger flows and specific risk areas is superior in promoting energy efficiency and enhancing passenger convenience, compared to broader management approaches.

Keywords energy efficiency, urban rail transit, public health emergency, targeted management, capacity utilization rate

1 Introduction

Public transport serves as a primary mode of transportation, facilitating accessibility to facilities and efficiently accommodating large passenger volumes with significantly lower per capita energy consumption compared to private vehicles (Qin and Liao 2021; Wang et al., 2021; Xie et al., 2021; He et al., 2022). However, during public health emergencies, such as the COVID-19 pandemic, passenger demand for public transport often declines, leading to a shift toward private cars, which may result in increased energy consumption and emissions (de Palma et al., 2022; Ji et al., 2022; Zhang et al., 2022). The physical mobility of individuals becomes a critical avenue for the spread of infectious diseases during public health emergencies. In the absence of adequate control measures or policies, maintaining recommended social distancing within public transport becomes challenging. Consequently, even minimal contact may contribute to contagion in enclosed public transport vehicles (Harris 2020). Therefore, the implementation of passenger flow control (PFC) measures in public transport becomes crucial for containing the spread and mitigating adverse effects during a public health emergency (Zhang et al., 2022; Sun et al., 2023).

In the post-pandemic era, where the threat of recurring outbreaks or seasonal infectious diseases with varying variants remains, a gradual restoration of public transport services and connectivity is essential to support economic activities (Zeng et al., 2021; Luo et al., 2023). Effective control measures for Urban Rail Transit (URT) services, including PFC, are necessary during public health emergencies (e.g., COVID-19) to manage the challenges posed by the emergency and address the high demand for travel. Neglecting this transition to the post-emergency

Received Sep. 4, 2023; revised Oct. 24, 2023; accepted Dec. 1, 2023

Kang HUANG
Integrated Research on Energy, Environment and Society (IREES), Energy and Sustainability Research Institute Groningen, University of Groningen, Groningen. 9747 AG, The Netherlands; Urban Planning and Transportation Group, Eindhoven University of Technology, Eindhoven., The Netherlands; School of Systems Science, Beijing Jiaotong University, Beijing 100091, China

Feixiong LIAO (✉), Soora RASOULI
Urban Planning and Transportation Group, Eindhoven University of Technology, Eindhoven., The Netherlands
E-mail: f.liao@tue.nl

Ziyou GAO
School of Systems Science, Beijing Jiaotong University, Beijing 100091, China

This work is jointly supported by the National Natural Science Foundation of China (Grant Nos. 72288101, 72101018, 72271127, 71801134) and the Dutch Research Council (NWO). The first author is grateful to the financial support by the China Scholarship Council (CSC).

phase may result in a significant mismatch between passenger demand and transport service supply, undermining transit-oriented development and carbon emission reduction efforts within the entire transport system. For instance, while transit operators may reduce the frequency or partially close URT lines to curb the spread of the virus, passengers often seek higher frequency and additional operation lines to maintain social distancing (Elias and Zatmeh-Kanj, 2021). Recognizing the indispensable interplay between demand and supply, effective control measures for URT services in the post-pandemic era are essential to harmonize the rebounding travel demand with pandemic containment efforts (Zhou and Koutsopoulos, 2021).

URT, as a major component of public transport, plays a pivotal role in reducing traffic congestion and carbon emissions by accommodating a substantial number of trips (Pan et al., 2018; Zhang et al., 2023). URT systems (Jia et al., 2021) have implemented a set of standardized operational procedures for public health emergencies, including pre-deployment of medical materials and equipment, categorization of emergencies and risk levels, analysis of specific operational measures, and the execution of effective protocols. On the one hand, URT operation is associated with elevated operational costs and energy consumption (Huang et al., 2017). Notably, in 2020, the Beijing Metro Company emerged as a major electricity consumer in Beijing, consuming over two billion kWh (Lv et al., 2019). On the other hand, ensuring social distancing within URT trains, which would typically be crowded, serves as an effective measure to curb the spread of the pandemic. Monitoring the train capacity utilization rate becomes crucial in facilitating social distancing among passengers. Consequently, while maintaining the highest possible train capacity utilization rate, the imposition of PFC is essential to achieve spatial and temporal redistribution of passengers. Remarkably, there is limited research that addresses energy efficiency objectives within a multi-line URT network and synchronization between passenger flow and timetable schedules (Kang et al., 2020). Therefore, as long as URT operations are not fully suspended, energy efficiency considerations should inform operations during public health emergencies.

To aid in the operational management of URT during a public health emergency, we propose a decision support model for energy-efficient line planning, integrating PFCs and train capacity utilization rate management. The variables of interest in this model are the train frequency for each URT line and the allocation of passenger paths. The primary objective of this decision support model is to minimize energy consumption while simultaneously regulating train capacity utilization rates on the tracks and minimizing passenger inconvenience when switching paths. While passenger safety is crucial during a public health emergency, we emphasize the importance of energy efficiency for two key reasons. First, energy consumption is closely tied to operational costs and can serve as a proxy objective for operational cost reduction, aligning with numerous energy-efficient optimization models (Canca and Zarzo, 2017; Huang et al., 2023). Secondly, energy efficiency should be reinstated as a regular objective once the public emergency situation transitions to a new normal phase. This is distinct from the initial stage of a public emergency when other objectives may take precedence (Wang et al., 2017; Gao and Yang, 2019).

For passengers who need to change their paths, we implicitly impose constraints on the additional travel time compared to their original paths (in the absence of control measures) during path generation preprocessing. This partially considers the objective of selecting paths with minimal travel times from the passenger's perspective. Specifically, assuming passenger arrivals at the train station (or entry rates) are regulated by a digital appointment system, we optimize the spatiotemporal distribution of passengers while adhering to desired train capacity utilization rates. These rates can be adjusted adaptively based on different risk levels during a public health emergency, with constraints targeted to zones of specific risk levels. This approach accounts for the geographical distribution of the emergency. To the best of our knowledge, this study represents the first exploration of PFC in the context of preventing the spread of a public health emergency while simultaneously considering URT energy efficiency and passenger convenience. We validate the proposed decision support model using real data from the COVID-19 outbreak in Xi'an, China, at the end of 2021. Our findings demonstrate that targeted PFC in high-risk zones effectively promotes social distancing and energy savings while keeping passenger inconvenience within acceptable limits. We also discuss various control policies for different pandemic stages, considering the trade-off between energy consumption and passenger inconvenience, as indicated by the number of Origin-Destination (OD) pairs affected by PFC.

The structure of this paper is organized as follows: Section 2 provides an in-depth exploration of the problem of energy-efficient line planning incorporating PFC within a URT network during a public health emergency, with a focus on COVID-19 as a special case. In Section 3, we develop a comprehensive decision support model for energy-efficient line planning, outlining assumptions, constraints, and the primary objective. Section 4 assesses the effectiveness of the proposed decision support model, and in Section 5, we investigate policy implications, draw conclusions, and outline future research directions.

2 PFC and energy efficiency in a URT network

To promote social distancing within train compartments,

reducing passenger capacity is a necessary approach. An example of this practice is illustrated in the "guidelines for zoning and grading control for COVID-19 in passenger hubs and vehicles" from the Ministry of Transport of China, which emphasizes strict control of train capacity utilization rates in high- and medium-risk zones. To effectively manage the spatiotemporal distribution of passengers, it is recommended that passengers reserve their rides before commencing their journeys. For instance, Beijing (China) has introduced the system of "subway by appointment" to control entry rates since 2020, as depicted in Fig. 1.

In this system, passengers are required to schedule their departure times, as shown in Fig. 1(a). For instance, a passenger planning to travel on May 16 can only book a trip for the following day. They receive a QR code and are assigned a specific entry gate to the boarding platform on their mobile phones. This QR code is valid for a 10 min window, as shown in Fig. 1(b). Passengers use the QR code to access the URT at the designated gate, where they wait while maintaining social distancing, as depicted in Fig. 1(c). Finally, passengers board the train and continue to observe social distancing, as shown in Fig. 1(d). According to a report, this system allows passengers to save an average of 3.5 min per trip compared to the scenario without an appointment system.

Fig. 1 Illustration of the appointment system of the Beijing URT.

Additionally, 57% of passengers adjust their departure times to minimize waiting time before boarding the trains (Wang et al., 2021). Without such a booking system and flow control measures, stations, especially transfer stations, and connected sections may become overcrowded (Guo et al., 2020).

Therefore, PFC or regulated path choice should be seamlessly integrated with controlled train capacity utilization rates. Different zones can be categorized by risk levels, such as high, medium, or low, with corresponding train capacity utilization rate limits enforced. It's important to note that the train capacity utilization rate serves as a valuable indicator for assessing passenger volume on the train and facilitating social distancing among passengers. This metric is relevant not only during post-emergency periods but also in regular scenarios. Given that energy efficiency is a fundamental objective in the daily operations of URT, the proposed decision support model remains applicable in typical operating conditions.

From the operator's perspective, the key decision variable to manage the service effectively and reduce the risk of infection while accommodating varying passenger demand is the train frequency (Ning et al., 2018). Combining the objectives of minimizing operational costs and mitigating negative environmental effects, maximizing energy efficiency (or minimizing energy consumption) is a pertinent operational goal. Hence, the primary objective of the proposed decision support model is to minimize energy consumption while adhering to constraints on train capacity utilization rates.

The decision support model relies on three sets of inputs, as illustrated in Fig. 2. First, the quota-based appointment module is utilized for PFC, outlining the maximum permissible passenger arrivals. In the process of generating alternative paths, long detour routes (e.g., those exceeding 1.5 times the shortest trip time) are excluded to prevent excessive passenger travel times (Huang and Liao, 2023). Through the appointment interface (as shown in Fig. 1), routes and entry points are recommended to passengers. Second, specific inputs include the risk level, time period, and affected zones, which are specified to determine the regulated utilization rates. Third, various parameters related to URT operations, such as speed profiles, train fleet size, and operation period, collectively determine a timetable. With these input data, passenger path allocation and train frequencies for all URT lines can be calculated within the optimization module, aligning with the energy efficiency objective in line planning. The passenger volume on each path and track is quantified, enabling the identification of bottlenecks at tracks or stations, which in turn informs decisions about train frequencies.

3 Decision support model

In this section, we introduce a decision support model designed for energy-efficient line planning within a URT network. The model framework integrates the management of passenger flow and train capacity utilization rates during a public health emergency. Herein, we outline the fundamental assumptions, constraints, and the primary objective of the model, which centers on energy efficiency.

Assumptions

In accordance with the problem description provided in Section 2, we establish several foundational assumptions for the decision support model. These assumptions are as follows:

Timetables: Timetables are designed in parallel and uniformly during an extended public health emergency period, such as the case with COVID-19. Timetabling primarily focuses on determining train frequencies during the tactical-level line planning stage (Mo et al., 2020).

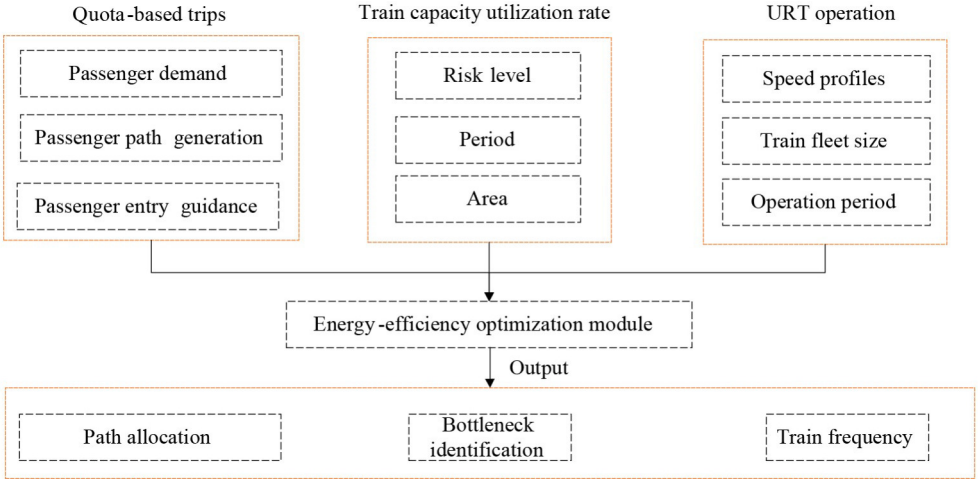

Fig. 2 Decision support model in regular response to public health emergencies.

Detailed timetabling at the operational level is not within the scope of consideration for this model. The key decision variable in the proposed model is the frequency of each URT line within the planning period. This frequency allocation plays a pivotal role in controlling and allocating passenger demand to various paths based on macro factors, including average waiting time, average transfer time, and fixed running times on each track. If there's a need to extend the model to the operational level, paths would need to account for micro factors, such as specific waiting times, transfer times, running times, and dwell times on each track, for time-independent passenger arrivals. Consequently, managing PFC at the operational level would involve complex details beyond the scope of the existing model. In essence, the proposed model has the potential for operational level extension.

Passenger Demand: Within the planning period, passenger demand is deterministic and originates from the appointment system. This appointment system closely resembles ticketing systems employed in the context of long-distance buses or trains. The URT line planning task is to transport all passenger demands, evenly distributed in a temporal sense, as facilitated by the appointment system. Consequently, the model is formulated within a static context, focusing on frequency-based URT planning.

Path Selection: In the absence of PFC measures, passengers would naturally opt for paths characterized by the lowest generalized costs. The generalized cost of a path may involve several components, including waiting time at initial platforms, transfer time (if applicable, including walking and waiting time), running time on tracks, dwell time at platforms, and ticket prices. Please note that the estimation or calibration of coefficients associated with these cost components falls outside the scope of this study.

Passenger Compliance: During a public health emergency, passengers are expected to strictly adhere to paths recommended by the operator, reflecting a full obedience rate (obedience rate equals 1). These recommended paths may not necessarily coincide with the minimum-cost paths, signifying that passengers prioritize safety over cost considerations.

Constraints

Three sets of constraints are involved in the decision support model for energy-efficient line planning regarding passenger path allocation, train capacity utilization rate, and the intensity of PFC.

Initially, it is crucial to uphold passenger path flow conservation within the URT network post path allocation. Passengers who require transfers to reach their destinations may have multiple alternative paths at their disposal. The existence of these alternative paths introduces opportunities for implementing PFC. Following passenger path allocation, the distribution of passenger volume q_{lt} on track t of line l, where a track refers to a line section between two neighboring platforms. We use x_{ui} to denote the proportion of passengers allocated to path i of OD pair u. The variables of concern in line planning are the passenger volumes on these tracks, representing the transportation of all passengers while averting stranding.

OD pairs fall into two distinct categories. First, OD pairs with only a single available path mean that passengers have no additional choice and have already been allocated to the available path. For this subset of OD pairs in the URT network, the passenger volumes on the tracks during the planning period, q_{lt}^0, are pre-calculated. Secondly, OD pairs with multiple alternative path, the corresponding set U_1 is considered for determining the total passenger volumes. To illustrate, consider the example in Fig. 3(a), depicting a network comprising four URT lines (two vertical and two horizontal lines). In this context:

The OD pair in which both the Origin (O) and Destination (D) are on the same URT line (denoted by the orange dotted line) features a direct train connection in orange (Fig. 3(b)). The OD pair involving O and D on different

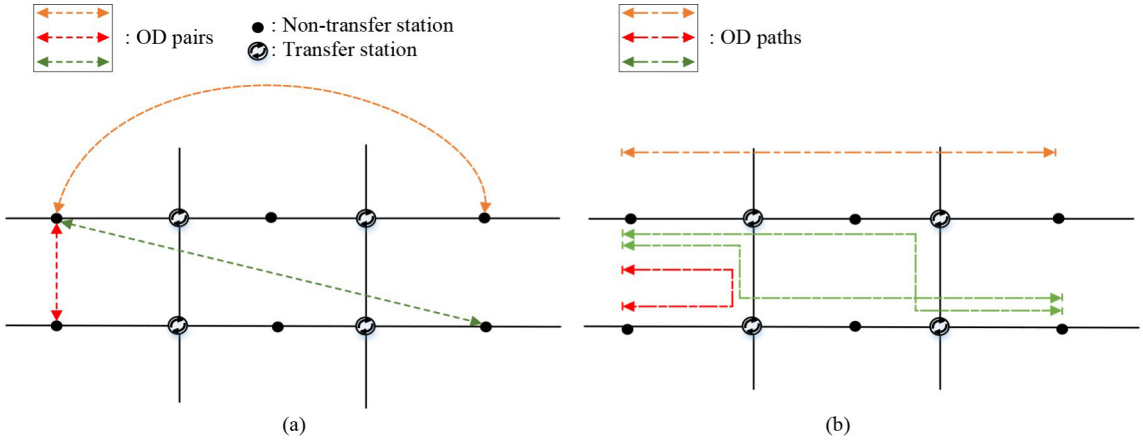

Fig. 3 Illustration of path allocation for different OD pairs.

URT lines (indicated by the red dotted line) has only one alternative path under consideration after eliminating long detours. The OD pair represented by the green dotted line requires a transfer and presents two alternative paths with comparable path costs. In a sparsely connected URT network, certain tracks may not be part of any cyclic path topologically. These tracks have no bearing on path allocation and thus entail straightforward flow loading calculations. However, the remaining tracks might be components of an alternative path for a specific OD pair, rendering them the focal point for path flow control. If a track is considered for the creation of an alternative path, T' is used to denote the subset of such key tracks for ease of communication. The path-track flow conservation can be formulated as Eqs. (1–3).

$$q_{lt} = q_{lt}^0 + \sum_{i \in I_u, u \in U} q_u^1 \cdot x_{ui} \cdot \lambda_{uilt}, \ \forall l \in L, t \in T', \tag{1}$$

$$\sum_{i \in I_u} x_{ui} = 1, \ \forall u \in U_1, \tag{2}$$

$$x_{ui} \in [0,1], \ \forall i \in I, u \in U_1, \tag{3}$$

where q_{lt} is the flow of track t on line l, q_{lt}^0 is the assigned passenger volumes on the track from the OD pairs without only one alternative path. T' is the set of key tracks in the URT network. q_u^1 is the allocated passenger demand of OD pair u with more than one alternative path. i and I_u are the index of the path and set of paths belonging to OD pair u. λ_{uilt} is a 0–1 parameter: $\lambda_{jilt} = 1$ if track t of line l is a part of path i of OD pair u; otherwise, $\lambda_{uilt} = 0$. x_{ui} is a proportion between 0 and 1 in Eq. (3).

The second set of constraints revolves around the regulation of train capacity utilization rates, which are designed to ensure the implementation of targeted social distancing measures. For each URT line, the frequency f_l of line l is determined by the track with the highest passenger volume, while maintaining the necessity of transporting all passengers. The maximum passenger volume $q_l^{\max}$ is the upper limit of passenger volume across all tracks, as outlined in Eq. (4). The train capacity utilization rate, influenced by path flow control measures, plays a critical role in determining and enforcing social distancing levels within the train. It's crucial to note that social distancing within a train differs from that observed in open spaces (e.g., maintaining a standard distance of 1 or 1.5 m). Instead, the train's capacity must align with the specified train capacity utilization rate φ for all tracks, as described in Eq. (5). Depending on the stage of the public health emergency, the mandatory train capacity utilization rate φ may be set at varying levels to meet the specific requirements of the situation.

For example, $\varphi = 0$ means a closedown of the URT system; PFC is implemented if $0 < \varphi < 1$; and $0 < \varphi < \varphi^{\max}$ refers to overloading, where $\varphi^{\max}$ is the maximum allowed train capacity utilization rate for safety considerations in normal operations. For the consideration of safety and capacity of the URT system, there is an upper bound constraint of frequencies of each line l, $f_l^{\max}$ in Eq. (6).

$$q_{lt} \leqslant q_l^{\max}, \ \forall l \in L, t \in T', \tag{4}$$

$$q_l^{\max} \leqslant f_l \cdot \gamma_l \cdot \varphi, \ \forall l \in L, \tag{5}$$

$$f_l \leqslant f_l^{\max}, \ \forall l \in L, \tag{6}$$

where γ_l is the train's full capacity of line l.

The third set of constraints focuses on regulating the intensity of PFC to prevent undue inconvenience to passengers. PFC measures must carefully balance operational costs with passenger inconvenience associated with deviating from their typical minimum-cost paths. Let α denote the maximum proportion of OD pairs for which passengers can be redirected from their minimum-cost paths to alternative paths. Since departing from the minimum-cost paths leads to passenger inconvenience and additional costs, α reflects the intensity of PFC. The scale of OD pairs that change their paths is constrained in Eq. (7), where y_u is a binary variable, $y_u = 1$ if any passengers of OD pair u change their paths from the minimum-cost path to other paths; otherwise, $y_u = 0$. x_{u1} is the proportion that the minimum-cost path is selected by passengers of OD pair u. The relationship between x_{u1} and y_u is formulated as Eq. (8). Constraints (6)–(7) can be transformed into the constraint of the scale of passengers switching from the minimum-cost paths to other paths.

$$\sum_{u \in U_1} y_u = |U_1| \cdot \alpha, \tag{7}$$

$$1 - x_{u1} \leqslant y_u, \ \forall u \in U_1. \tag{8}$$

Objective of energy-efficient URT

The traction energy in a URT system is consumed by the empty train and loaded passengers. Let E_l^1 and E_l^2 denote the decomposed energy consumption by the empty train and passenger weights of all tracks of line l, respectively. The total energy consumption can be calculated by summing up two parts: $\sum_{l \in L} f_l E_l^1$ and $\sum_{l \in L} f_l E_l^2$. The energy consumption by the empty train is the sum of energy consumption on all tracks of line l in Eq. (9) where e_{lt}^0 the base energy consumption of an empty train on track t of line l. According to the stable relationships between the energy consumption caused by passenger weights and empty trains, we formulate the total energy consumption based on the energy consumption by the empty train and a ratio θ between the two parts in Eq. (10). It should be noted that θ is related to the train capacity utilization rate φ. For instance, with train capacity utilization rate $\varphi = 1$ (full capacity), the ratio between $\sum_{l \in L} f_l E_l^2$ and $\sum_{l \in L} f_l E_l^l$ is approximately 1:3 (Huang et al., 2021). A

larger passenger loading (or train capacity utilization rate) results in a larger θ.

$$E_l^1 = \sum_{\forall t \in T_l} e_{lt}^0, \quad \forall l \in L, \tag{9}$$

$$E = \sum_{l \in L} f_l (E_l^1 + E_l^2) = \sum_{l \in L} f_l (1+\theta) E_l^1. \tag{10}$$

The outcome of the appointment system is the numbers of passengers allocated to the paths belonging to each OD pair. It is denoted by the decision variable x_{ui}. The train frequency f_l is the number of trains departing from one terminal to the other terminal of UTR line l, which is influenced by the constraint of the train capacity utilization rate. The train frequency influences the total energy consumption. The model objective of minimizing energy consumption is summarized as:

$$\begin{aligned} &\text{Min } E = \sum_{l \in L} f_l (1+\theta) E_l^1. \\ &\text{s.t. Eqs. } (1) - (9). \end{aligned} \tag{11}$$

The model utilizes Mixed Integer Linear Programming (MILP) with a manageable scale of variables and constraints. Solvers like Gurobi can be employed to find an exact solution within a reasonable computational timeframe. The primary objective of the model is to determine the train frequencies of the URT lines while refraining from modifying timetable elements such as running time and dwell time on each track. Consequently, this approach ensures that the minimum-cost paths within the URT network remain largely unchanged. Furthermore, during a public health emergency, passengers prioritize reaching their OD rather than seeking the path with the least generalized travel cost. This decision support model yields macroscopic parameters for evaluating a URT timetable under such circumstances, including average waiting time and transfer time, which are contingent on train frequency. To explore the microscopic effects, typically observed in normal operations, regarding precise waiting time and transfer time, the model should be expanded to include additional decision variables related to timetabling elements and account for the feedback loop between timetabling decisions and passenger path behavior, as discussed in the work of Huang et al. (2021).

Remark on model complexity

The number of variables and constraints in the decision support model are provided in Table 1. Four main factors determine the model complexity: (1) the number of OD pairs $|U_1|$ in the URT network, (2) the number of alternative paths, $\sum_{\forall u \in U_1} |I_u|$, which is related to the scale of the OD pairs, (3) the size of the set of key tracks $|T'|$, and (4) the number of lines in the URT network $|L|$. In a substantial URT network, when considering the model without any simplifications, it becomes a large-scale MILP problem. To mitigate the scale of variables and expedite computational efficiency, we can introduce two simplifications. First, through targeted management and control of risk zones, a key track may potentially serve as a representative bottleneck, including multiple tracks that lack transfer opportunities within a given path. $|T'|$ may only be a small part of the original tracks. Second, the OD pairs whose paths do not cover any key tracks can be ignored. Those OD pairs having overlapped path allocations can also be merged into one OD pair with the aggregated passenger demand in a simplified URT network. The scale of U_1 may only be a small part of the original OD pairs in real-world applications. With these reasonable simplifications, the optimization module in the decision support model can be solved with an exact optimal solution efficiently (e.g., a few seconds).

Table 1 Numbers of variables and constraints in the model ($|\cdot|$ is the size of a set)

Variables or constraints	Numbers
$f_l, E_l^1, E_l^2, q_l^{\max}$	$\|L\|$
Path proportion, x_{ui}	$\sum_{\forall u \in U_1} \|I_u\|$
Intermediate binary variable, y_u	$\|U_1\|$
Passenger volume on the track, q_{lt}	$\|T'\|$
Constraints (1), (4)	$\|T'\|$
Constraints (2), (8)	$\|U_1\|$
Constraints (3)	$\sum_{\forall u \in U_1} \|I_u\|$
Constraint (6)	$\|L\|$
Constraint (7)	1

Remark on targeted management

In adherence to the established standard operating procedure during a public health emergency, the URT operator initiates passenger path flow controls to facilitate targeted management. These controls are responsive to the varying risk levels observed in different zones. The intensity of passenger PFC includes several factors, including the total number of passengers permitted to access the URT system through the appointment system, the train capacity utilization rate (φ) on the tracks, and the train frequency of a given line (f_l). As an illustration, the guidelines for zoning and grading prevention and control of COVID-19 specify that the train capacity utilization rate in high- and medium-risk zones should be set at 0.5 and 0.7, respectively.

For dedicated passenger PFC policies, known as targeted management, it is essential to differentiate between zones based on their risk levels to avoid unnecessary adverse effects. According to the Coronavirus Pneumonia Prevention and Control Plan issued by China's State Council, low-risk zones impose no restrictions on train capacity utilization rates but mandate the wearing of masks. In contrast, high-risk zones enforce the lowest train capacity utilization rate. When a train travels from low-risk zones to higher-risk zones, the PFC strategy

involves diverting more passengers from their minimum-cost paths to alternative routes to comply with the specified train capacity utilization rate, resulting in reduced boarding rates in high-risk zones. Consequently, to account for zone-dependency, we should substitute Eqs. (4)–(5) with Eqs. (12)–(13).

$$q_{lt} \leqslant q_l^{\max}, \ \forall l \in L, t \in T^j, \ j \in J, \tag{12}$$

$$q_{lt} \leqslant f_l \cdot \gamma_l \cdot \varphi^j, \ \forall l \in L, t \in T^j, \ j \in J, \tag{13}$$

where j and J are the risk level and set of risk levels, $J = \{j \mid j = 1,2,\ldots,N\}$, T^j is the set of key tracks in the zones of risk level j, φ^j is the train capacity utilization rate during the emergency in the zones of risk level j, and N is the maximum risk level.

In summary, the decision support model for energy-efficient line planning serves as a versatile tool capable of offering optimal solutions for various objectives, including energy efficiency, train capacity utilization rate management to facilitate social distancing, and guidance for PFC implementation within an URT network.

4 Evaluation of the decision support model

The decision support model is applied to a practical case study involving a public health emergency, specifically the COVID-19 pandemic, to present its effectiveness. The study focuses on the City of Xi'an, the capital of Shaanxi province in North-west China, renowned for its development (Yin et al., 2021). The city boasts a medium-sized URT network structured in a square topology, comprising 4 lines, 94 stations (with 38, 42, 52, and 56 bidirectional platforms, respectively), and a total mileage of 158 km (additional details can be found in the Appendix of Huang et al., 2021). The maximum train fleet capacity for the URT network is 24 trains, each with a full capacity of 1762 passengers.

To streamline the URT network and manage overlapping path allocations for many OD pairs, the original network is simplified, as depicted in Figs. 4(a) and 4(b). The simplified network comprises representative tracks near transfer stations and includes 26 stations and 44 tracks. For Lines 1–4, the number of bidirectional tracks is reduced to 10, 12, 10, and 12, respectively. Alternative paths for each OD pair are generated using a k-minimum-cost path algorithm, with k = 3 chosen for this URT network. Paths with travel times exceeding 1.5 times that of the minimum-cost path are excluded.

Passenger demand data are sourced from the automatic fare collection system during the second stage of COVID-19 in 2021, simulating data from an envisioned appointment system. The analysis focuses on a one-hour time frame during non-peak hours when passenger demands in both up and down directions are relatively uniform. During this period, there were a total of 141,567 passenger trips, with 77% of these having multiple alternative paths.

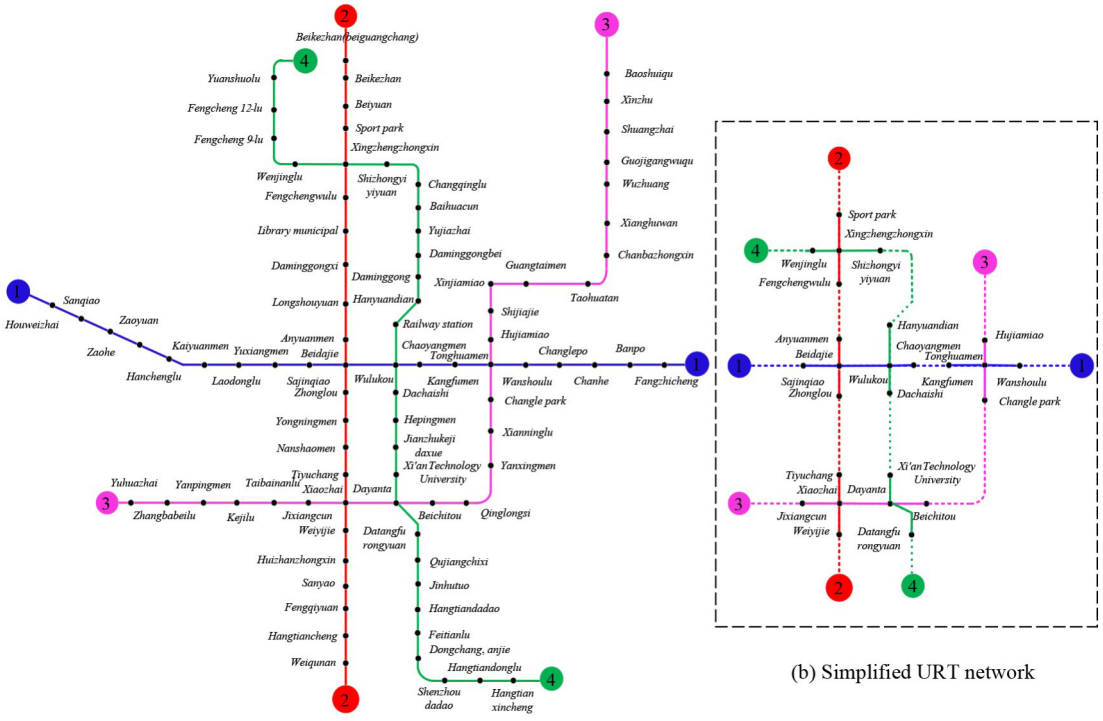

(a) Original URT network

(b) Simplified URT network

Fig. 4 Illustration of the simplified URT network.

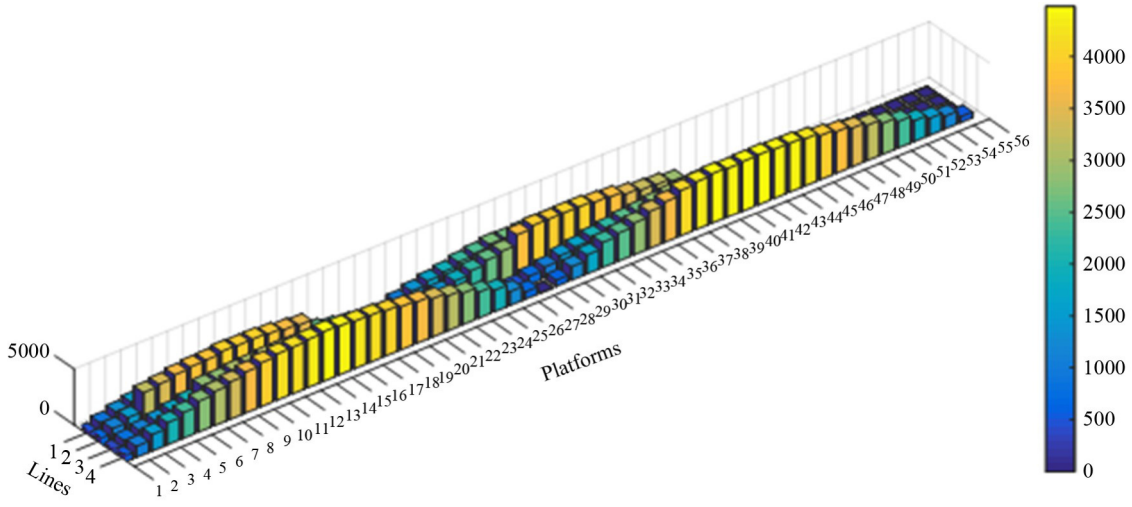

Fig. 5 Assigned passenger volume with only one valid path.

For OD pairs with only one path alternatively (comprising 23% of passenger trips), the passenger demands are directly assigned to the single paths.

Figure 5 illustrates the passenger volume distribution on each track, with larger volumes concentrated in the central segments of the URT lines, corresponding to areas with high business activity and facilities. Hourly passenger volumes in both up and down directions exhibit nearly symmetric patterns. The energy consumption (E_l^1) of empty trains for Lines 1 to 4 is as follows: 712.5, 792.5, 1063, and 1217.5 kWh, respectively, for the entire route based on the existing timetable.

The case study is based on the actual timeline of the COVID-19 outbreak in Xi'an at the end of 2021. The key events in the timeline are as follows:

On December 15, 2021, the first batch of confirmed COVID-19 cases was detected in Xi'an. The following day, an epidemiological survey led to the definition of several zones as medium-risk areas. As more confirmed cases were identified, the affected zones expanded. By December 19, 2021, the risk zones were further upscaled, and some were classified as high-risk areas. The risk zones remained in effect for approximately one and a half months, during which time no new confirmed cases were reported within 14 days. The risk zones were gradually deselected as the situation improved. The case study employs two scenarios to demonstrate the effectiveness of the proposed model framework: Case 1 assumes a scenario in which the utilization rate is set uniformly across all zones, representing comprehensive city-wide management ($t \in T'$). Case 2 examines the effect of zone-dependent φ to simulate targeted management.

The model is solved using Yalmip + Gurobi on a personal computer equipped with a Samsung 24 G RAM and Intel Core i7-8550U CPU. The computational time for solving the model is approximately 5 s, which is deemed acceptable for line planning, even without a real-time response requirement.

Case 1: A fixed train capacity utilization rate

The ratio θ between energy consumption caused by passenger weight and empty train is related to the train capacity utilization rate φ. A general relationship between θ and φ is supposed as $\theta = \varphi/3$ for calculating the total energy consumption. Passenger PFC plays a crucial role in regulating passenger volumes on URT tracks by adjusting the train capacity utilization rate. Since energy consumption calculations are based on the passenger load on each track, PFC significantly influences the energy consumption of URT operations. Optimized solutions with PFC at different φ ($\alpha = 100\%$) are presented in Table 2, along with a comparison to the energy efficiency associated with the original timetable without PFC, where all passengers choose the minimum travel time paths. Notably, when the train capacity utilization rate ($\varphi \leqslant 0.7$) is set at its highest level, the train capacity without PFC becomes insufficient to accommodate the passenger demand given the available fleet size. However, when PFC is implemented, passenger demand is met. Energy consumption experiences a significant reduction of approximately 36% across all tracks under PFC compared to the scenario without any path flow control. The effect of PFC on train frequencies for each line is evident in Fig. 6, with reductions observed across all cases. In summary, PFC leads to reductions in both train frequency and energy consumption.

Train frequencies are determined based on the passenger volume on the tracks. Taking $\varphi = 0.7$ for example, the passenger volumes on the key tracks with PFC are shown in Fig. 7, of which most are less than the scenario without path flow control. While certain tracks exhibit higher passenger volumes, the distribution of passenger volumes across tracks is more balanced with PFC. Consequently, PFC effectively mitigates peak passenger volumes for each line. It's worth noting that the key tracks consistently

Table 2 Energy consumption with different train capacity utilization rates φ

φ	θ	Optimized EC with PFC	EC without PFC	Energy reduction (%)
1	0.33	41607.72	65689.37	36.66
0.9	0.30	45134.70	70510.70	35.99
0.8	0.27	49345.85	78498.70	37.14
0.7	0.23	54298.97	86646.12	37.33
0.6	0.20	61963.80	NFS	NFS
0.5	0.17	72054.45	NFS	NFS
0.4	0.13	87026.39	NFS	NFS
0.35	0.12	101754.24	NFS	NFS
0.3	0.10	NFS	NFS	NFS

include those with the highest passenger volumes, which are identified as the bottlenecks (highlighted by the red arrow in Fig. 7) of the URT lines. These results affirm the sufficiency and efficacy of the selected key tracks.

The proportion of OD pairs influenced by the PFC has a direct effect on energy consumption. It's important to note that the control parameter α is equal to the allowed scale of OD pairs influenced by the PFC, expressed as a percentage of the total number of OD pairs. When α = 50%, 30%, and 10%, the allowed scales of OD pairs influenced by the PFC are 168, 101, and 34, respectively. This parameter indirectly affects the overall energy consumption.

As shown in Fig. 8(a), when $0.7 \leqslant \varphi \leqslant 1$, with increased allowed OD pairs that shift from the minimum-cost path to other paths, the energy consumption decreases. The minimum numbers of allowed OD pairs for train capacity utilization rates φ =1, 0.9, 0.8, and 0.7 are 168, 178, 184, and 207, respectively. Notably, stricter (lower) train capacity utilization rates necessitate more OD pairs to redirect passenger flow away from minimum-cost paths. Consequently, the inconvenience experienced by passengers who must change their paths increases as more energy is saved. When $0.35 \leqslant \varphi \leqslant 0.6$, without PFC, the

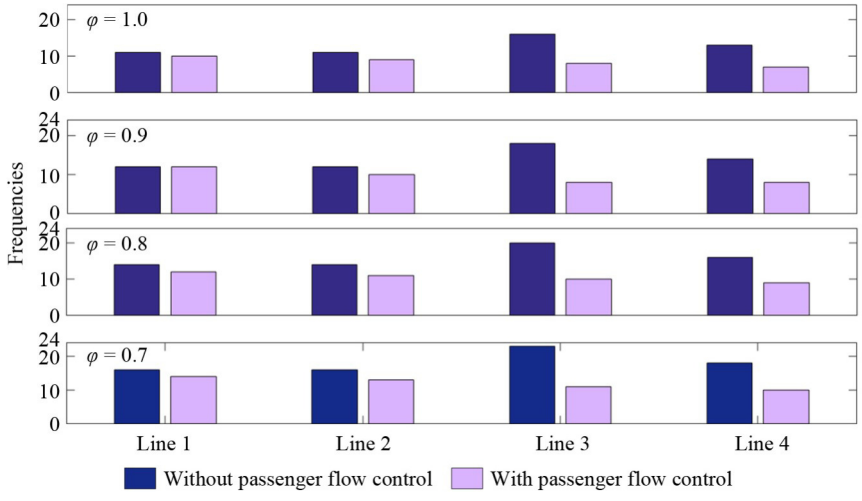

Fig. 6 Comparison of train frequencies with different train capacity utilization rates φ.

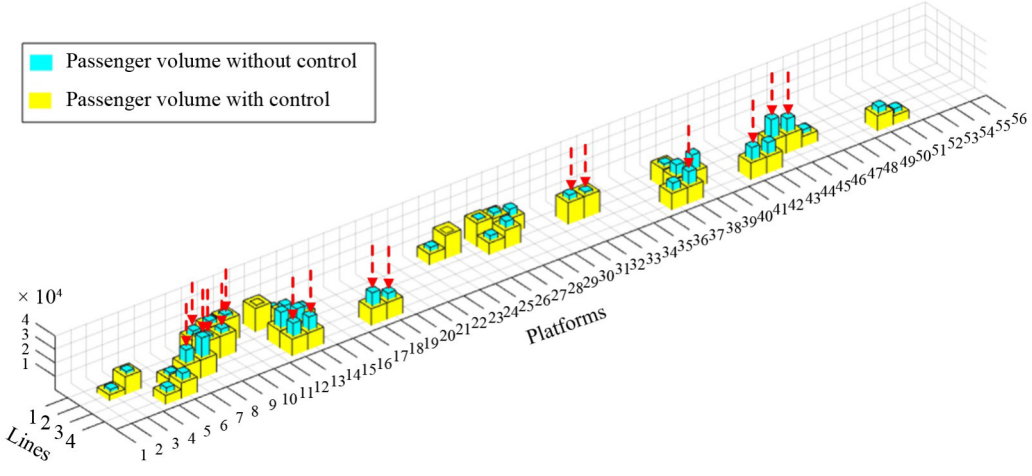

Fig. 7 Passenger volumes influenced by PFC.

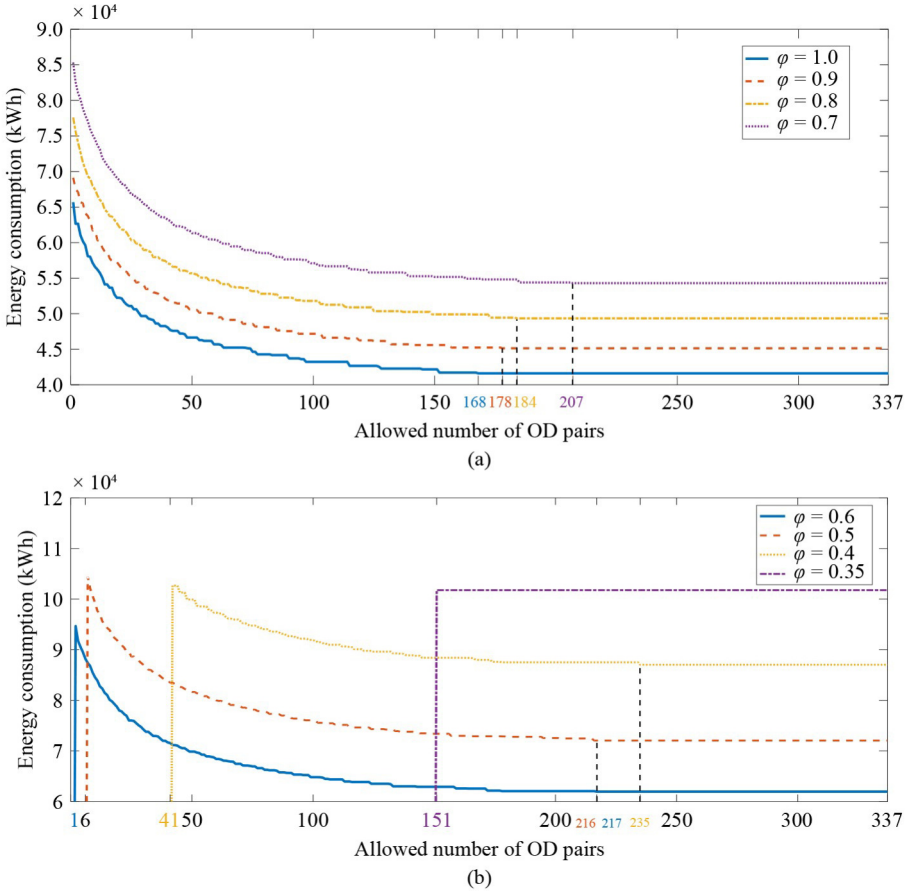

Fig. 8 The influence of the allowed scale of OD pairs by PFC. (a) Energy consumption varies with the scale of OD pairs influenced by PFC when $0.7 \leqslant \varphi \leqslant 1$. (b) Energy consumption varies with the scale of OD pairs influenced by PFC when $0.35 \leqslant \varphi \leqslant 0.6$.

train capacity is not enough to produce a feasible solution. As shown in Fig. 8(b), the solutions are not feasible when $\alpha = 0$. When more OD pairs are allowed for PFC, feasible solutions can be generated (e.g., 1, 6, 41, 151 for $\varphi = 0.6, 0.5, 0.4, 0.35$, respectively). The lower bound for the number of OD pairs is greater when the train capacity utilization rate is lower.

Case 2: Zone-dependent train capacity utilization rates

During the outbreak of COVID-19 in the City of Xi'an in 2021, there were two distinct stages, as illustrated in Fig. 9. In the first stage, two medium-risk zones, depicted within orange boxes and including eight key tracks, were identified. As the pandemic continued to spread and the number of confirmed cases increased, these two medium-risk zones were upgraded to high-risk zones, now indicated by the red boxes. Simultaneously, two new medium-risk zones with a total of four tracks were identified. The severity of the pandemic in the second stage surpassed that of the first stage.

To address the elevated risk levels, tracks connected to the risk zones were required to maintain lower train capacity utilization rates. Specifically, in the high-risk zones, the train capacity utilization rate was set at 0.5, while in the medium-risk zones, it was set at 0.7.

Using the decision support model, Table 3 provides information on energy consumption and train frequencies for each line during the first stage. If the entire city is designated as a medium-risk area without targeted management, energy consumption and train frequencies are higher. However, by focusing on the targeted risk zones, it is 68571.89 kWh, which means a 20.86% reduction in energy consumption compared to the scenario of setting medium-risk for the whole city (or (86646.12–68571.89)/86646.12). Meanwhile, with the implementation of PFC, energy consumption can be further reduced to 40330.47 kWh, equating to a 25.73% reduction compared to the case where the entire city is designated as medium-risk. Therefore, it is evident that PFC and targeted risk zone management are essential for conserving energy, enhancing transport capacity, and mitigating inconvenience in passenger path allocation.

The passenger volumes for key tracks on Lines 1 to 4 under different control policies are depicted in Fig. 10. When all key tracks in the entire city (the URT network) are designated as medium-risk zones ($\varphi = 0.7$), the passenger volumes on these tracks, when subject to PFC, consistently remain lower than those without PFC. Notably, the passenger volumes on key tracks within the

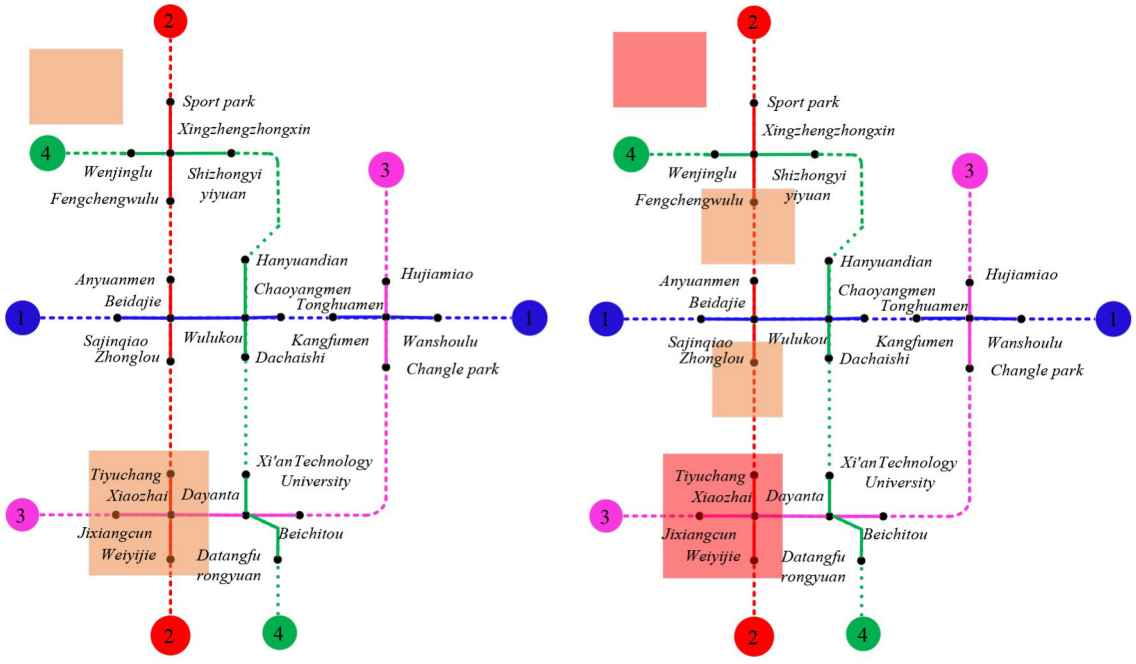

(a) Risk area at the first stage of the pandemic

(b) Risk area at the second stage of the pandemic

Fig. 9 Geographical distribution of COVID-19 in Xi'an in December 2021.

Table 3 Energy consumption and frequency at the first stage of the pandemic

Lines	Train frequencies			
	Medium-risk for the whole city		Medium-risk for the targeted zones	
	Without PFC	With PFC	Without PFC	With PFC
Line 1	16	14	11	11
Line 2	16	13	15	10
Line 3	23	11	19	8
Line 4	18	10	13	7
Total EC (kWh)	86646.12	54298.97	68571.89	40330.47
EC reduction with PFC (%)	NFS	37.33	NFS	41.19

Note: EC, energy consumption; NFS, no feasible solution.

targeted risk zone (highlighted in pink) are the lowest, as observed in Lines 2 and 3. This illustrates that with targeted management of the risk zones, it is possible to reduce passenger volumes in the risk zones without adversely affecting passengers in the non-risk zones, specifically the tracks on Lines 1 and 4.

During the second stage of the pandemic, when considering only the constraints for the risk zones, no feasible solution exists without PFC. With targeted risk zone management, the energy consumption is calculated at 43719.39 kWh. This represents a substantial 28.34% reduction in energy consumption when compared to the scenario of designating the entire city as high-risk. The energy consumption is influenced by the number of allowed OD pairs that are impacted by the PFC for both stages of the pandemic, as shown in Fig. 11. The minimum number of OD pairs requiring a shift in passenger flow from the minimum-cost path to other paths for the two stages is 223 and 176, respectively. It is worth noting that no feasible solution is attainable when the number of OD pairs allowing PFC falls below 2 during the second stage. Additionally, energy consumption increases with more and higher-risk zones, assuming the same travel demand and PFC parameters.

In summary, for a public health emergency such as COVID-19, where the train capacity utilization rate is crucial for implementing social distancing measures, the decision support model can identify the optimal line planning and passenger path allocation within the URT network. It's important to recognize the tradeoff between energy consumption and passenger inconvenience resulting from PFC. Targeted management of risk zones, as opposed to a broad approach covering the entire city, proves effective in reducing both energy consumption and the inconvenience faced by passengers when they need to deviate from their usual paths.

5 Discussion and conclusions

Building upon the insights gained from the case study, various control policies tailored to different stages of a

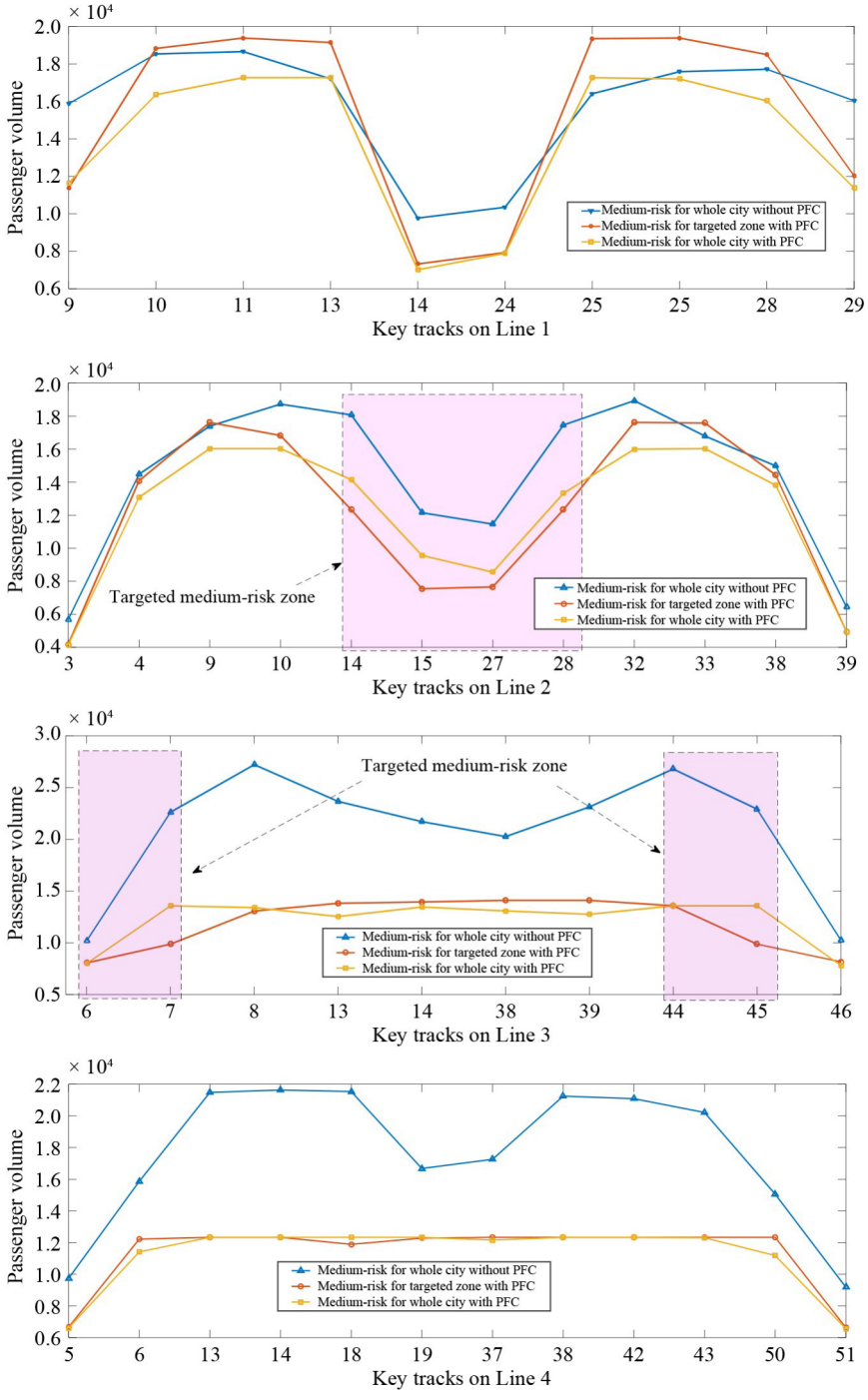

Fig. 10 Passenger volume influenced by PFC.

pandemic are deliberated. Furthermore, the subsequent section outlines the principal conclusions derived from the study and outlines potential directions for future research.

5.1 Policy implications

Based on the findings outlined in Section 4, the train capacity utilization rates on the tracks, the extent of risk zone coverage, and the intensity of passenger PFC significantly impact the energy consumption and transport capacity of the URT network. Consequently, policy implications are discussed along two key dimensions, as illustrated in Fig. 12.

In the first dimension, the spatial coverage of risk zones is categorized into global and target zones. The global zone pertains to management and control strategies spanning the entire city or larger administrative regions

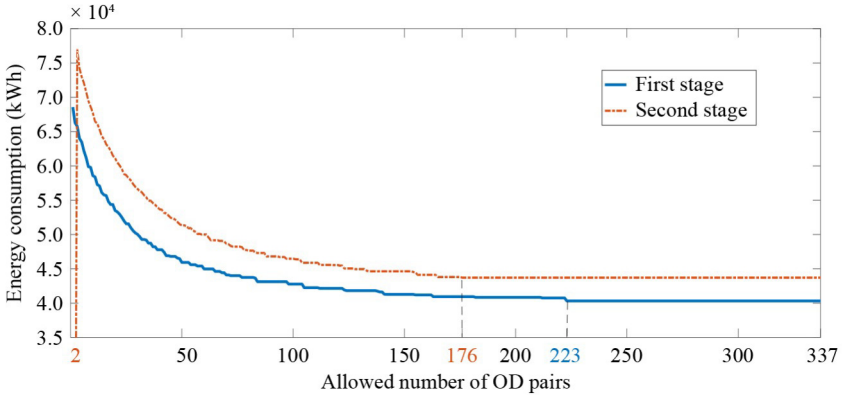

Fig. 11 Effects of the allowed scale of OD pairs influenced by PFC.

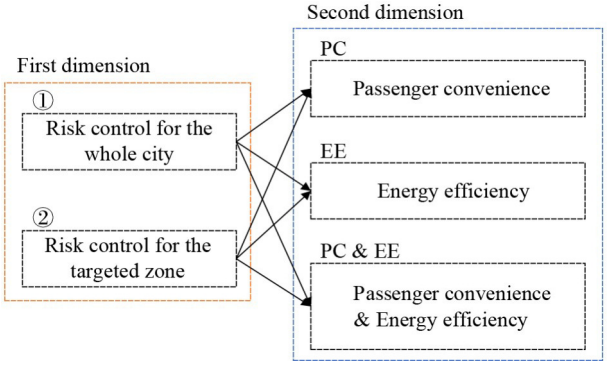

Fig. 12 Management and control policies for the public health emergency.

(①). In contrast, target zones refer to specific areas (②) distinguished by varying risk levels.

In the second dimension, taking into account distinct priorities in passenger convenience and energy efficiency, and adhering to the constraints specified in Eq. (7), three types of objectives are identified: passenger convenience-oriented (PC), energy efficiency-oriented (EE), and a balance between both (PC & EE). Consequently, six integrated and responsive PFC policies are proposed: ①-PC, ①-EE, ①-PC & EE, ②-PC, ②-EE, and ②-PC & EE (abbreviated as Policies A, B, C, D, E, and F, respectively). These control policies are applicable depending on the stage and priority of the public health emergency.

Policy A, for instance, entails low transport capacity to minimize passenger inconvenience during the initial outbreak of a public health emergency, such as the COVID-19 outbreak in Wuhan in 2020. This phase is characterized by an unclear understanding of the disease's transmission dynamics, and travel demand is significantly reduced primarily to essential mobility needs. Thus, the URT network can efficiently serve this reduced demand with lower-capacity supplies (Lu et al., 2022). As the travel demand gradually recovers and containment measures improve, the operator may transition to Policy B, which aims to save operational costs while still accommodating the relatively low travel demand. When travel demands start to rebound, Policy C is recommended to strike a balance between passenger convenience and energy efficiency, thereby maintaining ridership (Gkiotsalitis and Cats 2022). In essence, the decision support model, as demonstrated in Case 1 in Section 4, can provide URT network line planning solutions with PFC at varying train capacity utilization rates and levels of passenger inconvenience, enabling adaptive responses to different stages of a public health emergency.

As public health emergencies evolve, the negative effects, such as the number of confirmed cases, may decrease substantially due to large-scale vaccinations and seasonal effects. In such scenarios, where the emergency outbreaks are limited to specific local zones, the sustainability and necessity of global risk control measures may diminish. While it is unlikely that the risk of infection will be completely eliminated globally, especially in the presence of potential new variants of the virus, a deep understanding of the disease's transmission mechanisms allows for more targeted measures with fewer negative consequences for passenger convenience and operational costs. Drawing parallels to Policies A–C, Policies D–F center on the targeted management and control of risk zones, each with different objectives. Among these, Policy F stands out as it strikes a balance between passenger convenience and energy efficiency, making it particularly suitable for the post-pandemic era. The numerical results from Case 2 in Section 4 corroborate the superiority of targeted passenger PFC over extensive control in various performance indicators. In summary, under diverse public health emergency scenarios and with varying control objectives, the decision support model, along with its potential extensions, proves invaluable for optimizing URT operations effectively.

5.2 Conclusions and future work

The public health emergency presents significant challenges for the management and control policies of public transport systems. To mitigate the negative effects of

such emergencies in URT systems, this paper has developed a decision support model focused on energy efficiency. This model determines optimal train frequencies and passenger PFC while adhering to train capacity utilization rate constraints. Formulated as a MILP, the model has proven to be effective, as demonstrated in the case study involving the COVID-19 outbreak in Xi'an at the end of 2021. The results highlight the model's ability to reduce energy consumption while considering the tradeoff with passenger inconvenience resulting from path flow control.

Several potential avenues for future research based on the proposed model framework are worth exploring. First, investigating other operational measures such as stop-skipping and partial station closures in risk zones may offer additional strategies to prevent the spread of pandemics. Second, considering the unique context of a public health emergency, where passengers are required to make appointments and follow guided paths, introducing a compliance rate as a factor in PFC and allowing for passenger choice in some cases could be a valuable extension. This approach would involve calculating passenger volumes on tracks for both passengers who comply with path control and those who do not. Third, for passengers with complex multimodal trip chains and activities, integrating coordination between URT and other transport modes is an essential aspect to explore (Liao et al., 2014; Liao, 2021). Finally, considering network topology as a factor influencing the spread of pandemics and energy consumption is a promising direction for future research.

Competing Interests The authors declare that they have no competing interests.

References

Canca D, Zarzo A (2017). Design of energy-efficient timetables in two-way railway rapid transit lines. Transportation Research Part B: Methodological, 102: 142–161

de Palma A, Vosough S, Liao F (2022). An overview of effects of COVID-19 on mobility and lifestyle: 18 months since the outbreak. Transportation Research Part A, Policy and Practice, 159: 372–397

Elias W, Zatmeh-Kanj S (2021). Extent to which COVID-19 will affect future use of the train in Israel. Transport Policy, 110: 215–224

Gao Z, Yang L (2019). Energy-saving operation approaches for urban rail transit systems. Frontiers of Engineering Management, 6(2): 139–151

Gkiotsalitis K, Cats O (2022). Optimal frequency setting of metro services in the age of COVID-19 distancing measures. Transportmetrica A: Transport Science, 18(3): 807–827

Guo X, Wang D Z, Wu J, Sun H, Zhou L (2020). Mining commuting behavior of urban rail transit network by using association rules. Physica A, 559: 125094

Harris J E (2020). The subways seeded the massive coronavirus epidemic in New York City. National Bureau of Economic Research

He J, Yan N, Zhang J, Yu Y, Wang T (2022). Battery electric buses charging schedule optimization considering time-of-use electricity price. Journal of Intelligent and Connected Vehicles, 5(2): 138–145

Huang K, Liao F (2023). A novel two-stage approach for energy-efficient timetabling for an urban rail transit network. Transportation Research Part E, Logistics and Transportation Review, 176: 103212

Huang K, Liao F, Gao Z (2021). An integrated model of energy-efficient timetabling of the urban rail transit system with multiple interconnected lines. Transportation Research Part C, Emerging Technologies, 129: 103171

Huang K, Liao F, Lyu H, Gao Z (2023). Assessment of the tradeoff between energy efficiency and transfer opportunities in an urban rail transit network. Sustainable Energy Technologies and Assessments, 58: 103360

Huang Y, Yang L, Tang T, Gao Z, Cao F (2017). Joint train scheduling optimization with service quality and energy efficiency in urban rail transit networks. , 138: 1124–1147

Ji J, Bie Y, Zeng Z, Wang L (2022). Trip energy consumption estimation for electric buses. Communications in Transportation Research, 2: 100069

Jia J, Chen Y, Wang Y, Li T, Li Y (2021). A new global method for identifying urban rail transit key station during COVID-19: A case study of Beijing, China. Physica A, 565: 125578

Kang L, Sun H, Wu J, Gao Z (2020). Last train station-skipping, transfer-accessible and energy-efficient scheduling in subway networks. , 206: 118127

Liao F (2021). Exact space–time prism of an activity program: bidirectional searches in multi-state supernetwork. International Journal of Geographical Information Science, 35(10): 1975–2001

Liao F, Arentze T, Timmermans H (2014). Multi-state supernetworks: recent progress and prospects. Journal of Traffic and Transportation Engineering, 1(1): 13–27

Lu Y, Yang L, Yang K, Gao Z, Zhou H, Meng F, Qi J (2022). A distributionally robust optimization method for passenger flow control strategy and train scheduling on an urban rail transit line. Engineering, 12: 202–220

Luo Q, Forscher T, Shaheen S, Deakin E, Walker J L (2023). Impact of the COVID-19 pandemic and generational heterogeneity on ecommerce shopping styles—A case study of Sacramento, California. Communications in Transportation Research, 3: 100091

Lv H, Zhang Y, Huang K, Yu X, Wu J (2019). An energy-efficient timetable optimization approach in a bi-direction urban rail transit line: A mixed-integer linear programming model. Energies, 12(14):

2686

Mo P, Yang L, D'Ariano A, Yin J, Yao Y, Gao Z (2020). Energy-efficient train scheduling and rolling stock circulation planning in a metro line: A linear programming approach. IEEE Transactions on Intelligent Transportation Systems, 21(9): 3621–3633

Ning J, Zhou Y, Long F, Tao X (2018). A synergistic energy-efficient planning approach for urban rail transit operations. Energy, 151: 854–863

Pan D, Zhao L, Luo Q, Zhang C, Chen Z (2018). Study on the performance improvement of urban rail transit system. Energy, 161: 1154–1171

Qin J, Liao F (2021). Space-time prism in multimodal supernetwork-Part 1: Methodology. Communications in Transportation Research, 1: 100016

Sun X, Wandelt S, Zhang A (2023). Why are COVID-19 travel bubbles a tightrope walk? An investigation based on the Trans-Tasmanian case. Communications in Transportation Research, 3: 100089

Wang L, Yang L, Gao Z, Huang Y (2017). Robust train speed trajectory optimization: A stochastic constrained shortest path approach. Frontiers of Engineering Management, 4(4): 408–417

Wang Q, Guo J, Ge Y, Liang C, Xian K, Diao J, Zhang L, Ma Y (2021). Practice and thoughts on reservation travel in Beijing Metro Stations. Urban Transp. China, 19: 89–94

Xie J, Zhang J, Sun K, Ni S, Chen D (2021). Passenger and energy-saving oriented train timetable and stop plan synchronization optimization model. Transportation Research Part D, Transport and Environment, 98: 102975

Yin J, Cao X J, Huang X (2021). Association between subway and life satisfaction: Evidence from Xi'an, China. Transportation Research Part D, Transport and Environment, 96: 102869

Zeng G, Sun Z, Liu S, Chen X, Li D, Wu J, Gao Z (2021). Percolation-based health management of complex traffic systems. Frontiers of Engineering Management, 8(4): 557–571

Zhang L, He D, He Y, Liu B, Chen Y, Shan S (2022). Real-time energy saving optimization method for urban rail transit train timetable under delay condition. Energy, 258: 124853

Zhang P, Yang X, Wu J, Sun H, Wei Y, Gao Z (2023). Coupling analysis of passenger and train flows for a large-scale urban rail transit system. Frontiers of Engineering Management, 10(2): 250–261

Zhou J, Koutsopoulos H N (2021). Virus transmission risk in urban rail systems: microscopic simulation-based analysis of spatio-temporal characteristics. Transportation Research Record: Journal of the Transportation Research Board, 2675(10): 120–132